



Designing of a novel heterogeneous catalyst comprising 12-tungstophosphoric acid and zeolite HY for the synthesis of bio-based esters

Anjali Patel¹ · Margi Joshi¹ · Shivani Sharma¹

Received: 28 May 2022 / Revised: 27 August 2022 / Accepted: 31 August 2022 / Published online: 13 September 2022
© The Author(s), under exclusive licence to Springer-Verlag GmbH Germany, part of Springer Nature 2022

Abstract

The present work consists of development of a novel heterogeneous catalyst comprising Keggin type polyoxometalate, 12-tungstophosphoric acid (PW_{12}), and zeolite HY and its evaluation for the synthesis of alkyl levulinate. Various physico-chemical methods were used for characterization, and the reaction optimization was studied by applying the impacts of the main reaction parameters (i.e. catalyst loading, molar ratio of acid to alcohol, time, and temperature). The catalyst shows 88% conversion and 99% selectivity towards n-butyl levulinate under optimized conditions such as 90°, 8 h with molar ratio of acid to alcohol (1:2) following second-order kinetics with activation energy of 80 kJ/mol. The catalyst is recovered and reused three times, always showing good performances. The catalyst was also found to be versatile and sustainable for a number of different bio-platform molecules, and alcohols with different chain lengths give % selectivity of respective esters between 49 and 100%. A comparison with the reported ones having phosphotungstate-based heterogeneous catalysts as well as classical ion-exchange resins shows superiority of the present catalyst in terms of lower amount (0.025 g) as well as highest TOF of 425 h⁻¹.

Keywords 12-Tungstophosphoric acid · Zeolite HY · Sustainable catalyst · Bio-fuel additive · n-Butyl levulinate

1 Introduction

Expanded use of nonrenewable petroleum resources causes an urgent need of development of new technologies for the utilization of renewable resources in the production of chemicals, fuels, and energy [1]. Biomass — the only renewable abundant carbon natural source which is broadly available, is propitious regarding this as it is a sustainable and possible resource for the production of chemicals and fuels. From the industrial as well as environmental perspectives, the conversion of biomass derivatives to their value-added chemicals has gained much importance. It is already known that hydrolysis of cellulose and hemicellulose leads to sugar formation whose catalytic conversion can attain to the formation of platform chemicals like 5-hydroxymethylfurfural,

levulinic acid, and furfural [2], and levulinic acid (LA) is viewed as one of the most favourable building blocks for the biomass refinery [3].

By securing a place in the top twelve value-added chemicals from biomass, levulinic acid provides itself as starting material for exploring more value-added chemicals including angelica lactones, 2-methyltetrahydrofuran, δ -aminolevulinic acid, γ -valerolactone, alkyl levulinates, succinic acid, and pyrrolidines have numbers of applications [4, 5]. The presence of two functional groups — ketone and carboxylic acid in levulinic acid, makes it an important building block chemical. Alkyl levulinates are the top most desirable products in view of their valuable applications such as biofuels/bio-lubricants and also in the fragrance industries. Amongst n-butyl levulinates are interestingly on focus and used as flavouring agents, food contact, cosmetics, polymer precursors, and fuel additive. Their high miscibility in diesel even at the diesel cloud point (247 K), high lubricity, and conductivity and non-toxic nature are noteworthy [6].

Due to the said importance, number of heterogeneous catalysts is developed for synthesis of n-butyl

✉ Anjali Patel
anjali.patel-chem@msubaroda.ac.in

¹ Polyoxometalates and Catalysis Laboratory, Department of Chemistry, Faculty of Science, The Maharaja Sayajirao University of Baroda, Vadodara 390020, Gujarat, India

levulinate such as supported montmorillonite [7], zeolites [8, 9], metal–organic frameworks [10], silicas [11–13], mesoporous materials [14–16], ion-exchange resins [17, 18], graphene oxide [19], titania nanotubes [20, 21], enzymes [22], immobilized lipase [23, 24], polymers [25], magnetic nanoparticles [26], and supported heteropolyacids (HPAs) [27–32]. Amongst all, the contribution from HPA-based catalysts, especially Keggin type, is found to be excellent from the viewpoint of their compositions and varied structural properties. Keggin type of HPAs is Bronsted acids, having metal–oxygen octahedra with general formula $[XM_{12}O_{40}]^{n-}$, where X is the heteroatom (P or Si) and M is the addenda atom (Mo, W, V, etc.) and are excellent homogeneous catalysts [33]. However, due to the known demerits of homogeneous catalysts, having low surface area, as well as solubility in polar media, makes a separation of reaction mixture uneasy. The said disadvantages are overcome by making them heterogeneous via using suitable supports, leading to high surface area, high catalytic activity as well as selectivity, and mainly the regeneration of the catalyst. Towards the same, until the date, MCM-41 [31], silicalite-1 zeolite [28], and MCM-22 [30] have been used to make HPAs heterogeneous catalysts for the synthesis of n-butyl levulinate. It is interesting to note down that instead of having number of advantages, zeolite HY has not been explored as a support for 12-tungstophosphoric acid.

Zeolites are microporous crystalline aluminosilicates commonly composed of aluminium, silicon, and oxygen. Compared to natural zeolites, synthetic zeolites such as A, β , X, and Y have the widespread commercial applications. Acidity is a prime parameter of zeolites, and it arises from the unbalanced charge between alumina and silica units which alternate inside the continuous crystalline aluminosilicate framework. Zeolite HY explores the known importance like it is made up of an intergrowth of two or more polymorphs comprising a three-dimensional system of 12-membered ring channels. It has a free diameter of 6–8 Å, large pore size, large surface area, large pore volume, high thermal and chemical stability, and the presence of surface silanol groups. Hence, it was selected in the present study. It is well known that zeolites possess higher Lewis acidic sites and shows lower Brønsted acidic sites available on the surface [34–36]. Keeping this in mind, to increase the Brønsted acid sites, we have selected 12-tungstophosphoric acid for the same as it has strongest Brønsted acidity in the Keggin heteropolyacid series.

The main objectives of the present work are as follows:

- (1) To combine the advantages of the high Bronsted acidity of 12-tungstophosphoric acid and the three-dimensional porous system of zeolite
- (2) To develop reaction system to upgrade renewable biomass, one of the main goals of green chemistry
- (3) To use the solid acid catalysts, instead of noble metals, with the possibility to upscale catalytic process by avoiding corrosion and waste liquid acid separation.

In this work, 12-tungstophosphoric acid (PW_{12}) was anchored to zeolite HY by wet incipient impregnation method. Both support and catalyst were characterized for acidity as well as by various physicochemical methods such as BET, EDX, TGA, FT-IR, XRD, and NMR. The catalytic performance was evaluated for esterification of bio-platform molecule, and levulinic acid, with n-butanol by varying different parameters. The kinetics experiment was carried out, and the activation energy was determined for the said reaction. The catalyst was regenerated, and its characterization was carried out to verify its sustainability. The esterification of different bio-platform molecules and alcohols having different chain lengths was carried out to explore the versatility of the present catalyst. Finally, the focus on uniqueness of present catalyst was made by comparing it with the reported catalysts.

2 Experimental

2.1 Materials

All chemicals used were of A. R. grade. 12-tungstophosphoric acid (extra pure), ammonium chloride (99%), adipic acid (99%), succinic acid (99.5%), fumaric acid (99.5%), malonic acid (99%), lauric acid (99%), n-butanol (> 99%), 1-propanol (> 99%), 2-butanol (> 98%), isopropyl alcohol (> 98%), tert-butanol (> 98%), 1-butanol (> 98%), 1-pentanol (> 99%), 1-hexanol (> 99%), 1-octanol (> 99%), 2-octanol (> 98%) and dichloromethane (> 99%) were used as received from Merck. Levulinic acid (> 98%) was acquired from Avra Synthesis Pvt. Ltd. Palmitic acid (98%) was acquired from Loba Chemie. Zeolite NaY was obtained commercially from Reliance Industries Limited, Vadodara, Gujarat.

2.2 Synthesis of the catalysts

2.2.1 Step 1: Conversion of NaY to its protonic form zeolite HY (ZHY)

Zeolite NaY was converted into the ammonium form NH_4Y , by conventional ion-exchange method [37]. One gram of zeolite NaY and 100 mL of 1 M NH_4Cl solution were taken in a 250 mL round bottom flask and refluxed at 80 °C for 2 h. The solution was cooled, filtered, washed with distilled water, and dried at 120 °C for 4 h. The above procedure was

repeated for 2 times to get complete exchange of sodium cation Na^+ to ammonium cation NH_4^+ . The resulting zeolite NH_4Y was further calcined in air at $550\text{ }^\circ\text{C}$ for 5 h to introduce it in a protonic form (H^+). The obtained material was designated as zeolite HY (ZHY).

2.2.2 Step 2: Anchoring of PW_{12} to zeolite ZHY

Synthesis of a series of catalysts comprising 10–40% of PW_{12} was carried out by the incipient wet impregnation method (Scheme 1). One gram of zeolite HY was suspended in an aqueous solution of PW_{12} (0.1 g/10 mL to 0.4/40 mL in distilled water). After stirring it for 5 h, the suspension was dried in oven at $100\text{ }^\circ\text{C}$ for 10 h. The obtained catalysts were designated as $(\text{PW}_{12})_1/\text{ZHY}$, $(\text{PW}_{12})_2/\text{ZHY}$, $(\text{PW}_{12})_3/\text{ZHY}$, and $(\text{PW}_{12})_4/\text{ZHY}$, respectively.

2.3 Characterization

2.3.1 Acidity measurements

Acidic properties of support and catalysts were determined by n-butylamine titration and potentiometric titration method.

Total acidity by n-butylamine titration method A 0.025-M solution of n-butylamine in toluene and 0.025 M trichloroacetic acid in toluene were prepared for the assessment of

total acidity of the catalysts [38]. The 0.25 g catalyst was suspended in 25 mL n-butylamine solution for 24 h, and the excess base was titrated against trichloroacetic acid-toluene solution using neutral red as an indicator. Total acidity was calculated from the following equation.

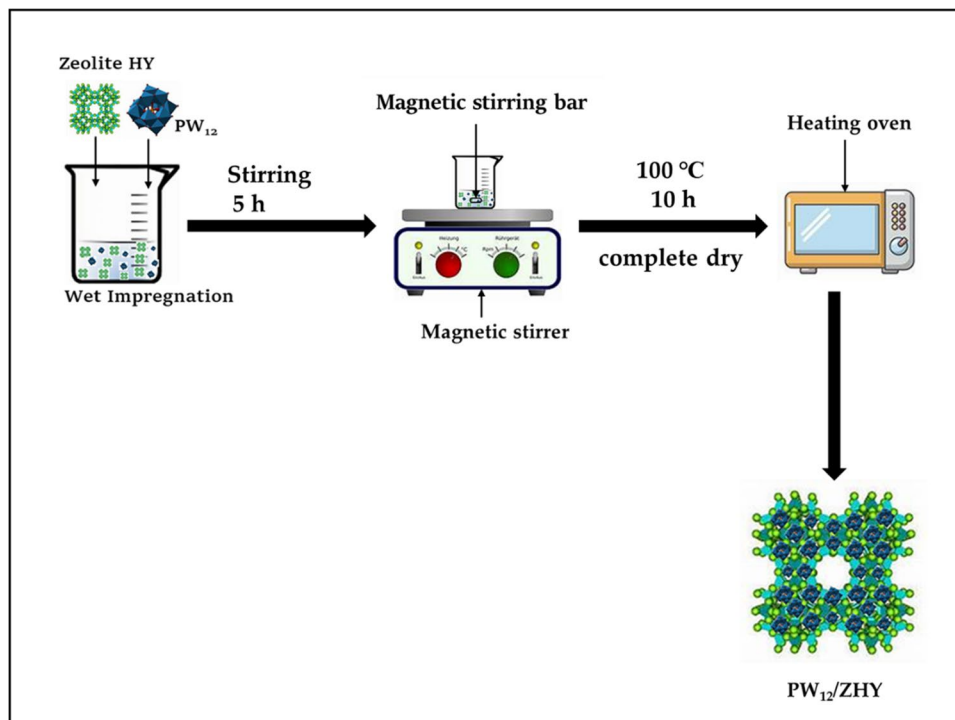
$$\text{Acidity (mmol/gm)} = \frac{\text{gm of n-butylamine (used in titration)}}{\text{molecular weight of n-butylamine}}$$

Potentiometric titration method A suspension of 0.25 g of catalyst/support was prepared in 25 ml of acetonitrile, stirred for about 12–15 min, and initial electrode potential was measured (which indicates its acidic strength). To this suspension, 0.05 M n-butylamine solution in acetonitrile (0.1 ml) was added and allowed to stir for 3 h at $25\text{ }^\circ\text{C}$. Then potentiometrically, it was titrated against the same solution of n-butylamine, and the variation in electrode potential was noted with a digital pH metre. The acidic sites were assigned according to the following scale: $E_i > 100\text{ mV}$ (very strong sites), $0 < E_i < 100\text{ mV}$ (strong sites), $-100 < E_i < 0\text{ mV}$ (weak sites) and $E_i < -100\text{ mV}$ (very weak sites) [39].

2.3.2 Physicochemical methods

The N_2 adsorption–desorption isotherms (at 77 K) and BET (Brunauer–Emmett–Teller) surface area measurements were carried out using Micromeritics ASAP 2010 (USA)

Scheme 1 Synthesis of the catalyst by wet impregnation method



volumetric static adsorption instrument. The calculations of pore size distributions were done through the BJH adsorption–desorption method. The JSM-7100F EDX-SEM analyser was used for the elemental analysis. Thermogravimetric analysis (TGA) was carried out on the Mettler Toledo Star SW 7.01 under the nitrogen atmosphere with a flow rate of 2 mL min⁻¹ at 25–600 °C (ramp rate of 10 °C min⁻¹). The Fourier transform infrared (FT-IR) spectra of the sample were obtained in the range 4000–400 cm⁻¹ by using KBr disc on Shimadzu instrument (IRAffinity-1S). The powder X-ray diffraction (XRD) patterns for the samples were recorded using Philips PW-1830 instrument in the 2θ range 5–90° (Cu Kα radiation λ = 1.54 Å). The solid-state ³¹P MAS NMR spectra were recorded on JOEL ECX 400 MHz high-resolution multinuclear FT-NMR spectrometer.

2.4 Catalytic reactions

The reaction was carried out in a 50 mL batch reactor. Levulinic acid (10 mmol, 1.16 g), n-butanol (20 mmol, 1.48 g), and the catalyst (25 mg) were charged into the batch reactor equipped with an air condenser, guard tube, and magnetic stirrer. The reaction mixture was heated at desired temperature and time with continuous stirring. After completion, the reaction mixture was cooled to room temperature and dilute with 15 mL of dichloromethane (DCM), and centrifugation was done. The reactants and products were analysed by a gas chromatograph GC-FID (Shimadzu-2014) using a capillary column RTX-5 (internal diameter: 0.25 mm, length: 30 m). It was carried out according to the following temperature profile: initially, the oven temperature was set at 35 °C, then the temperature increased from 35 to 300°, with a total flow of 9.1 mL/min, and finally to 300 °C with a total flow of 50 mL/min. The initial pressure was 69.4 kPa which will increase up to 100 kPa. Throughout, the purge flow remained 3.0 mL/min. On the basis of obtained GC analysis, the % conversion (on the basis of levulinic acid) and % selectivity were calculated from the following equation:

$$\% \text{ Conversion} = \frac{\text{initial mol \%} - \text{final mol \%}}{\text{initial mol \%}} \times 100$$

$$\% \text{ Selectivity} = \frac{\text{moles of product formed}}{\text{moles of substrate consumed}} \times 100$$

2.5 Leaching and hot filtration test

The leaching of PW₁₂ from the support was checked by following the same procedure reported in literature [40]. Qualitative determination of heteropoly acids can be done by treating it with a mild reducing agent such as ascorbic acid, giving heteropoly blue colouration. One gram of PW₁₂

loaded ZHY was suspended and kept in 10 ml water for 24 h. The supernatant solution was then decanted and treated with ascorbic acid solution. The leaching of PW₁₂ was also checked in the residue obtained after the reaction by hot filtration test. After the completion of reaction, the reaction mass was filtered hot, and the obtained filtrate was treated with the solution of ascorbic acid.

2.6 Kinetic study

A detailed kinetic study was carried out in a temperature range of 70 to 100 °C at time intervals of 4, 6, and 8 h (under optimized conditions with > 50% conversion) as well as at lower time intervals, i.e. 0.5, 1, 1, 5, 2, and 3 h (with < 50% conversion) by using the same reaction pathway and methodology used in optimization of main reaction parameters. For each temperature, the rate constant was calculated graphically for 1st order [log a(a-x) vs time] as well as for 2nd order (1/(a-x) vs time where (a-x) represents concentration). The activation energy was calculated by plotting graph of lnk vs 1/temperature.

2.7 Regeneration study

For regeneration of catalyst, the reaction was carried out in optimized reaction parameters by using the same pathway that was applied in the optimization of reaction parameters. After the first cycle, the reaction mixture was diluted with DCM, and the catalyst was separated by centrifugation method. The collected catalyst was then washed with 5 ml of fresh methanol, followed by water, and dried in an oven at 100 °C for 2 h, designated as R-PW₁₂/ZHY and employed for the next cycle. The schematic representation of regeneration of catalyst is shown below (Scheme 2).

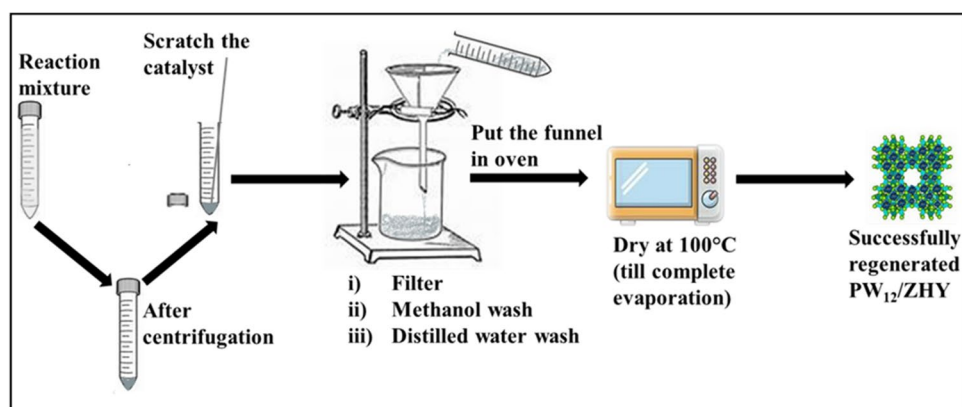
2.8 Relative activity of different substrates

The esters formed via different substrate studies have a large importance in the industry as well as in fuel blending. Hence, the synthesis of various esters using different bio-derived acids and alcohols were performed by using the same methodology and reaction parameters that were optimized in the synthesis of n-butyl levulinate.

3 Results and discussion

3.1 Catalyst characterization

The acidity of catalysts and support was measured by n-butylamine titration method. Firstly, the physical appearance was observed in the colour change from yellow to pink. The obtained acidity results are enumerated in Table 1.

Scheme 2 Regeneration of synthesized catalyst**Table 1** Acidity measurement of support and catalysts

Materials	Potentiometric titration				n-Butylamine titration		
	Acidic strength (mV)	Types of acidic sites (meqg ⁻¹)			Total no. of acidic sites (meqg ⁻¹)	Total no. of acidic sites (mmolg ⁻¹)	Total acidity (mmolg ⁻¹)
		Very Strong	Strong	Weak			
NaY	192	0.2	0.2	1.1	1.5	0.30	0.25
ZHY	289	0.4	0.4	2.5	3.3	0.66	0.83
(PW ₁₂) ₁ /ZHY	510	2.2	1.9	1.5	5.6	1.12	1.00
(PW ₁₂) ₂ /ZHY	517	3.0	2.0	2.3	7.3	1.46	1.40
(PW ₁₂) ₃ /ZHY	525	3.4	2.4	2.0	7.8	1.57	1.57
(PW ₁₂) ₄ /ZHY	528	3.3	1.7	3.0	8.0	1.60	1.60

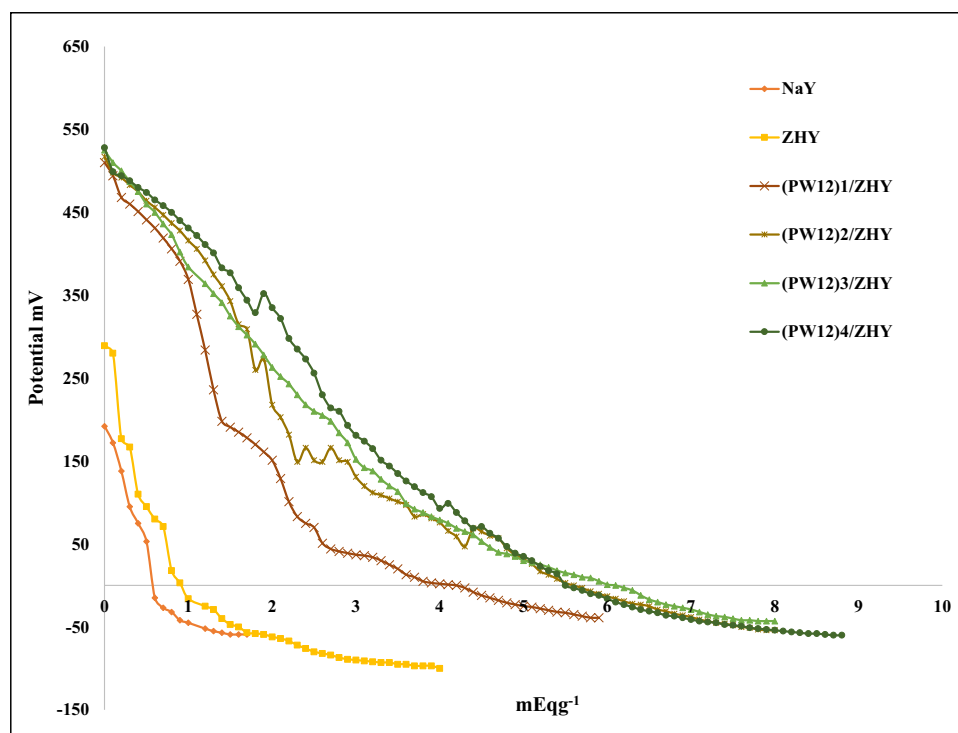
NaY shows the acidity 0.25 mmol/g. The increase in acidity (0.83 mmol/g) after treatment of NH₄Cl indicates successful exchange of sodium cation by the protons. The acidity of catalysts was increased with the increase in % loading of PW₁₂. This observation is due to the fact that with increase in % loading of PW₁₂, the Brønsted acidic sites in the catalyst increase, and hence, the total acidity increases. The higher values of acidity of the catalysts as compared to that of ZHY confirmed the successful impregnation of PW₁₂ into ZHY. However, no appreciable increase in acidity was found from 30 to 40% which may be because of the blocking of the Brønsted acidic sites of the catalyst. This is attributed to the fact that the availability of more acid sites will favour the increase in the probability of contact of molecules on the surface of the catalyst [30]. The higher availability of active sites may facilitate the reverse reaction. Hence, 30% loading was found to be optimum.

The obtained acidic strength as well as acidic sites for all materials, determined by potentiometric titration, is enumerated in Table 1, while the change in the electrode potential as a function of mEq per grams of n-butylamine is shown in Fig. 1. Higher acidic strength of the catalyst may be due to the introduction of PW₁₂. Furthermore, it is also seen that with increase in loading of PW₁₂ from 10 to 30%, the acidic sites also increase, which is in good agreement with the fact

that being a Brønsted acid, it is expected in enhancement of acidity as well as the acidic strength. However, with further increase in the % loading to 40%, a negligible change was observed which may be because of the blocking of the Brønsted acidic sites of the catalyst [30]. Hence, 30% loading was optimized.

Textural properties of support as well as catalysts are shown in Table 2. With increase in % loading of PW₁₂, BET surface area as well as pore volume and pore diameter decreases which suggests the incorporation as well as anchoring of PW₁₂ inside ZHY. Furthermore, when % loading increased from 30 to 40%, no appreciable change was observed in the surface area as well as pore diameter and pore volume. Therefore, 30% loading was optimized, and (PW₁₂)₃/ZHY was selected for further studies. It is renamed as PW₁₂/ZHY. The nitrogen adsorption–desorption isotherms of ZHY (Fig. 2.) shows type-1 isotherm with H1 hysteresis loop, a characteristic of microporous material [41]. PW₁₂/ZHY shows similar isotherm indicating no structural changes in the basic structure of ZHY after anchoring of PW₁₂ as well as successful filling of pores of ZHY.

The results of elemental analysis by EDX mapping are shown in Table 3 and Fig. 3. The values obtained from EDX are in good agreement with the theoretical values indicating successful impregnation of PW₁₂.

Fig. 1 Potentiometric titration curves of support and catalysts**Table 2** Textural properties of support and catalysts

Material	Surface area (m ² /g)	Pore diameter (Å)	Pore volume (cm ³ /g)
NaY	609	20.5	0.024
ZHY	560	20.8	0.034
(PW ₁₂) ₁ /ZHY	445	21.9	0.021
(PW ₁₂) ₂ /ZHY	391	20.5	0.019
(PW ₁₂) ₃ /ZHY	330	20.6	0.018
(PW ₁₂) ₄ /ZHY	326	20.4	0.016

The TGA of pure PW₁₂ (Fig. 4a) shows first weight loss of 16% appearing at temperature lower than 130 °C which corresponds to loss of adsorbed water molecules. The second weight loss of 4.67% was observed between 130 and 250 °C due to loss of crystalline water molecules, and the final weight loss of 3.73% up to 550 °C corresponds to decomposition of Keggin unit into the simple oxides [42]. The TGA of ZHY (Fig. 4b) shows first weight loss of 20% between a temperature range of 60 to 150 °C linked to the dehydration of the water adsorbed, physically/chemically, on the surface of the material [43]. The second loss of 6.01% in the temperature range of 150 to 250 °C corresponds to the elimination of water molecules produced by the dehydroxylation of silicate and aluminium [43, 44]. The observed last weight loss of 3.63% up to 550 °C may be due to the presence of impurities. However, no any significant weight

loss after 250 indicates the stability of the ZHY at higher temperature. TGA of PW₁₂/ZHY (Fig. 4c) shows weight loss in two steps. Initially, weight loss of 20.01% was observed up to 150 °C due to the loss of adsorbed water molecules, whereas the second and third weight loss (2.99% and 2%) between 150 and 550 °C correspond to the loss of the crystalline water molecules present in Keggin unit and support's impurity respectively. No further sharp weight loss indicates stability of the catalyst at higher temperature.

FT-IR spectra of PW₁₂, ZHY, and PW₁₂/ZHY are shown in Fig. 5. ZHY shows broadband at 3433 cm⁻¹ corresponds to hydroxyl group of Si–OH bonds. The most intense band of ZHY corresponding to the internal Si–O(Si) and Si–O(Al) asymmetric stretching vibrations of primary structural units, i.e. SiO₄ and AlO₄ tetrahedra, is located at 1145 cm⁻¹ and 1057 cm⁻¹, respectively, while the bands at 785 cm⁻¹ and 578 cm⁻¹ correspond to symmetric stretching vibrations of Si–O–Si and Si–O–Al bridges, respectively [41]. The typical bands for PW₁₂ are observed in PW₁₂/ZHY are 1080 cm⁻¹ and 897 cm⁻¹ due to P–O stretching and W–O–W asymmetric stretching, respectively [30, 45]. The presence of these bands reveals that the primary structure of PW₁₂ Keggin unit is preserved in the synthesized catalyst. The absence of other bands may be due to the superimposition with that of the bands of ZHY in the same region at 982 and 821.

The powder XRD patterns for PW₁₂, ZHY, and PW₁₂/ZHY are shown in Fig. 6. The diffractograms of ZHY showed intense reflections at 2θ = 6.55°, 10.3°, 11.3°,

Fig. 2 Nitrogen adsorption–desorption isotherms of **a** ZHY and **b** PW_{12}/ZHY

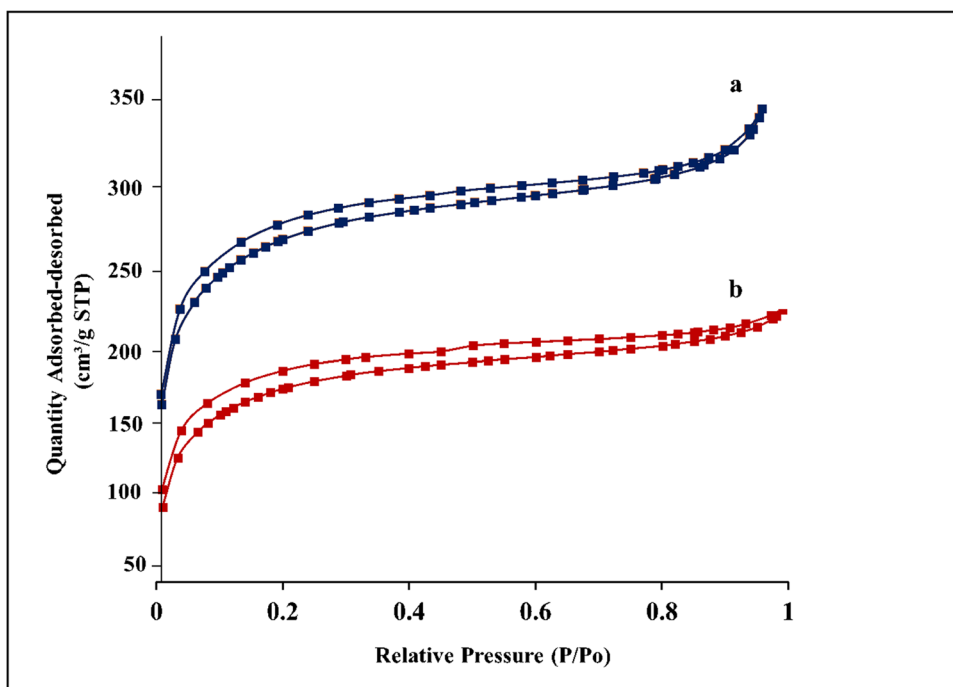
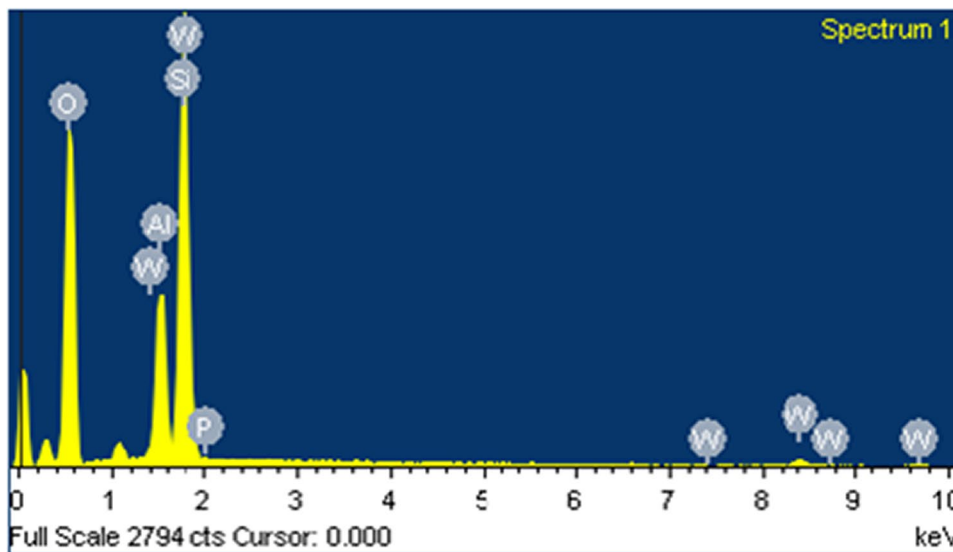


Table 3 Elemental analysis of PW_{12}/ZHY

Material	Si (wt%)	O (wt%)	Al (wt%)	P (wt%)		W (wt%)	
				By EDX	Theoretical	By EDX	Theoretical
PW_{12}/ZHY	21.24	53.56	7.41	0.23	0.24	17.48	17.56

Fig. 3 EDX mapping of PW_{12}/ZHY



15.8°, 17.6°, and 23.7°; 27.7° corresponds to (111), (220), (311), (331), (511), (533), and (553) planes [46]. The X-ray diffraction pattern of PW_{12}/ZHY was found to be similar to the ZHY indicating the zeolite framework is not affected by the impregnation of PW_{12} . On the contrary, no characteristic diffraction peaks related to PW_{12}

were observed which suggests its well dispersion inside the pores of ZHY.

The ^{31}P MAS NMR spectra of PW_{12} and PW_{12}/ZHY are presented in Fig. 7. PW_{12} shows chemical shift at -15.626 ppm (inset), and it is in good agreement with the reported value [47]. The catalyst, PW_{12}/ZHY , shows

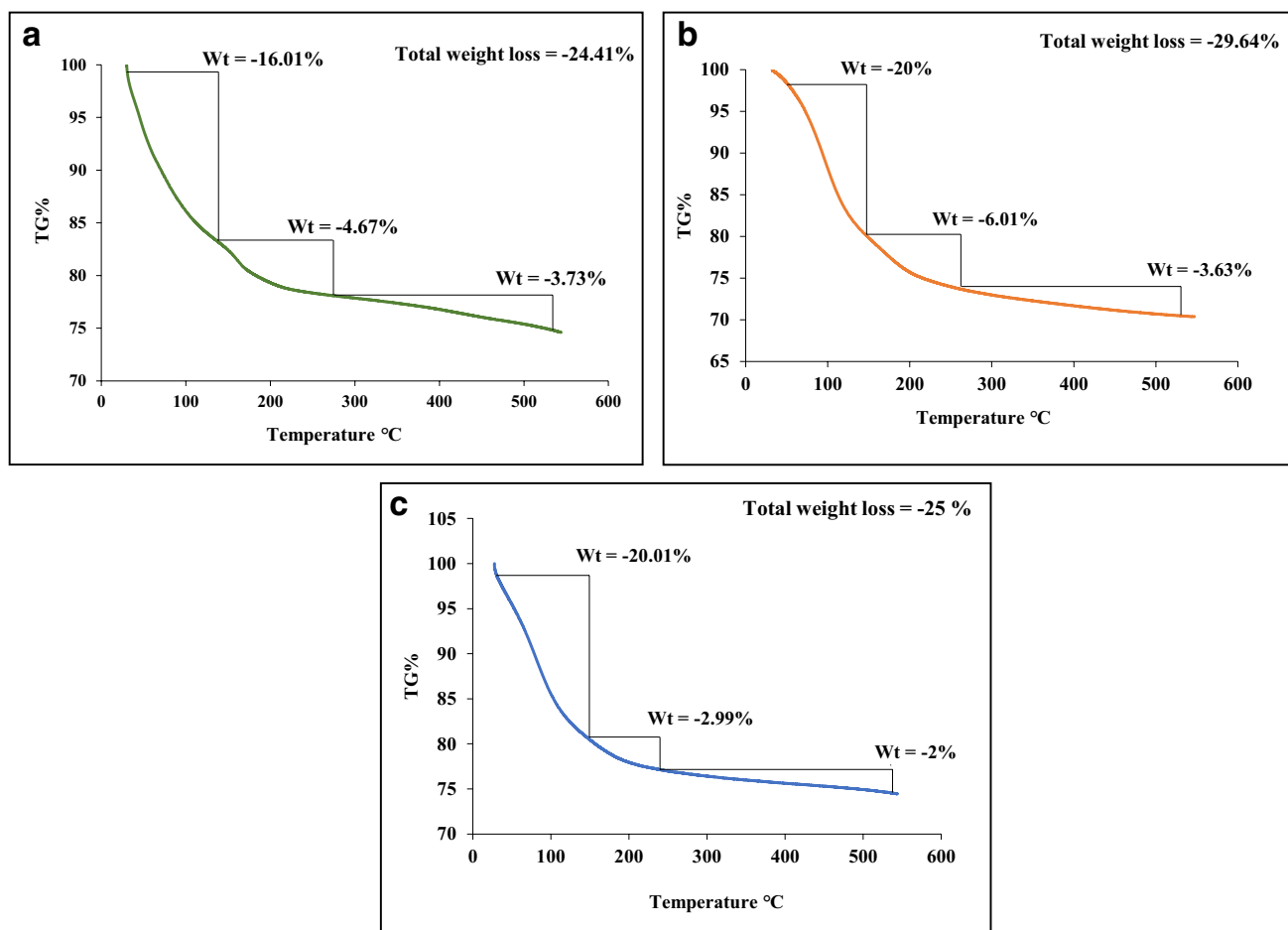


Fig. 4 a TGA plot of PW_{12} . b TGA plot of ZHY. c TGA plot of PW_{12}/ZHY

chemical shift at -12.484 ppm. The observed change in the chemical shift can be attributed to the strong interaction of PW_{12} with ZHY as well as partial dehydration of PW_{12} [48].

3.2 Catalytic performance

The esterification of levulinic acid with n-butanol (Scheme 3) was studied in detail by varying different parameters such as % loading of PW_{12} , mole ratio of levulinic acid to n-butanol, temperature, catalyst amount, and time to achieve maximum % conversion of levulinic acid.

First of all, influence of % loading of PW_{12} on the conversion was studied (Fig. 8a). It was observed that the reaction progresses well with the increase in the amount of PW_{12} from 10 to 30%, in good agreement with the values of acidic sites/strength (Table 1). Inversely, in case of 40% PW_{12} , it decreases, may be due to the blocking of active sites which restrict the reactant molecules to access more active catalytic sites to the availability of more acid sites, which favours the increase in the probability of contact of molecules on the

surface of the catalyst [49]. The higher availability of active sites may facilitate the reverse reaction. Hence, the catalyst consist of 30% loading of PW_{12} was selected to study other reaction parameters.

Figure 8b shows the effect of mole ratio of levulinic acid to n-butanol (1:1 to 1:3), and the results clearly revealed that initially increase in mole ratio from 1:1 to 1:2 leads to increase in % conversion from 64 to 88% as well as the selectivity of ester. Further increase in the mole ratio to 1:3, the % conversion significantly decreased to 81% with almost no difference in selectivity of ester. This may assign to the higher viscosity of the solution which will slow the mass transfer. On the other hand, the increase in the amount of n-butanol in reaction media increases the dilution which may lead to the in situ esterification followed by pushing the equilibrium to the product [49]. Hence, % conversion reduced. The mole ratio of 1:2 was selected looking to maximum 88% conversion.

The effect of catalyst amount was studied by varying the amount between 25 and 75 mg as shown in Fig. 8c. Obtained results show that with increase in catalyst amount, % conversion

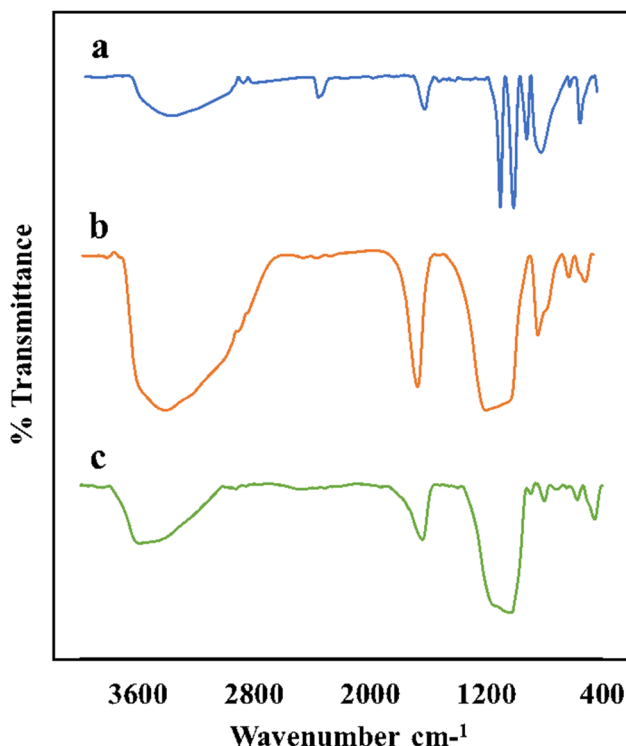


Fig. 5 FT-IR spectra of **a** PW_{12} , **b** ZHY, and **c** PW_{12}/ZHY

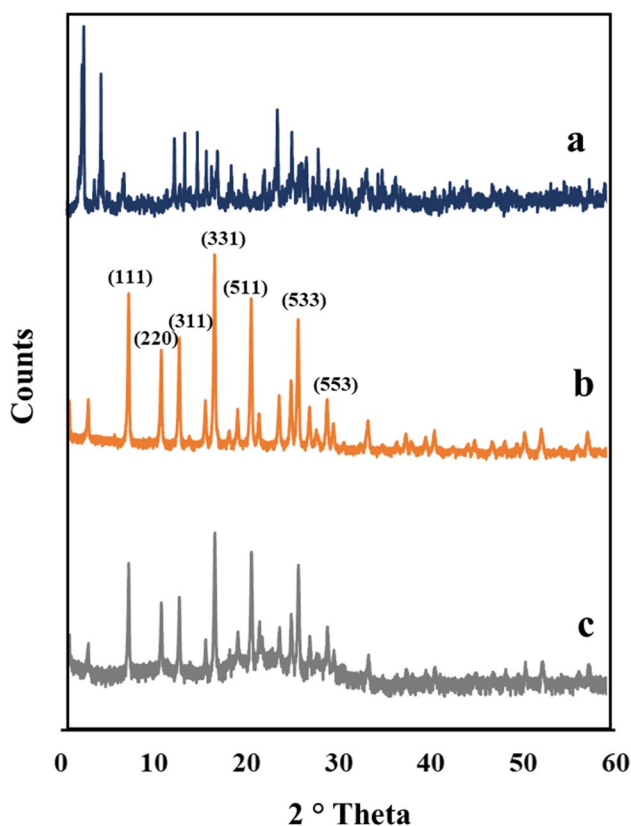


Fig. 6 XRD spectra of **a** PW_{12} , **b** ZHY, and **c** PW_{12}/ZHY

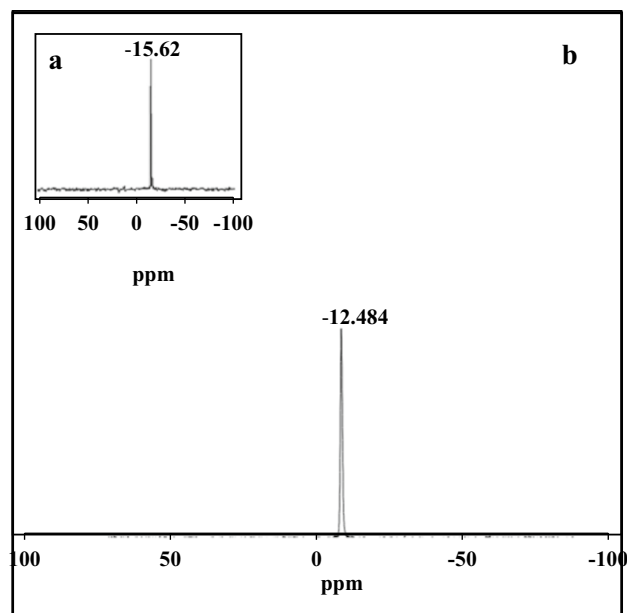


Fig. 7 ^{31}P MAS NMR spectra of inset. **a** PW_{12} and **b** PW_{12}/ZHY

also increases up to 50 mg which is in good agreement with the known fact that the higher catalyst amount leads to higher active sites which will increase the rate of conversion. Maximum 93% conversion was achieved by using 50 mg of the catalyst. However, % conversion and selectivity readily decreased for 75 mg. The reason behind decreased conversion pointed out the increase in mass density due to solvent-free reaction [50]. Accordingly, 25 mg of catalyst amount is optimized.

To study the influence of temperature, reaction was screened for a range from 70 to 110 °C, and the obtained results are presented in Fig. 8d. With increase in temperature from 70 to 90 °C, % conversion increased tremendously from 60 to 88%. This may be due to the fact that the esterification reaction is endothermic, and it endorses reaction equilibrium in forward direction at higher temperature as well as increase in the collisions between reactant molecules and catalyst. However, at 100 °C, a negligible change was observed in the % conversion as well as selectivity of ester. After that, the catalytic activity was also studied at higher temperature, i.e. 110 °C, and nearly complete conversion (99%) with 100% selectivity was achieved. Keeping in mind the industrial aspects (energy saving), 90 °C was considered optimal as achieving higher temperature is also an energy-demanding process.

The effect of time was also studied between 2 and 12 h with interval of 2 h as shown in Fig. 8e. The gradual increase in % conversion was observed from 45 to 88% with increase in time initially up to 8 h. The increased time allowed the esterification reaction to proceed more thoroughly. Respectively, the selectivity for esters also increased from 89 to 99%. With further increase in time, the reaction may precede in backward direction as expected that ester decomposes to form

Scheme 3 Esterification of levulinic acid and n-butanol

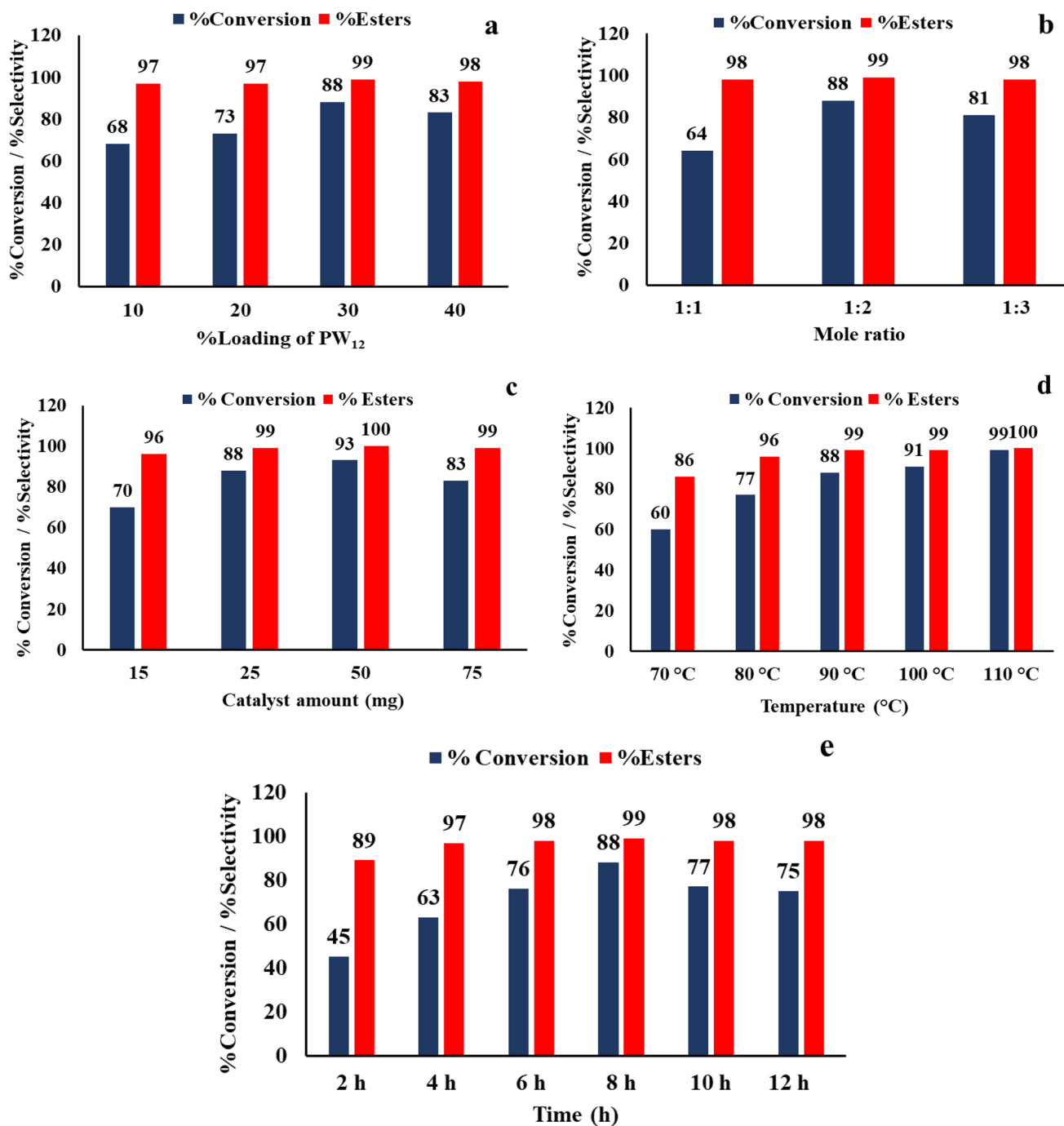
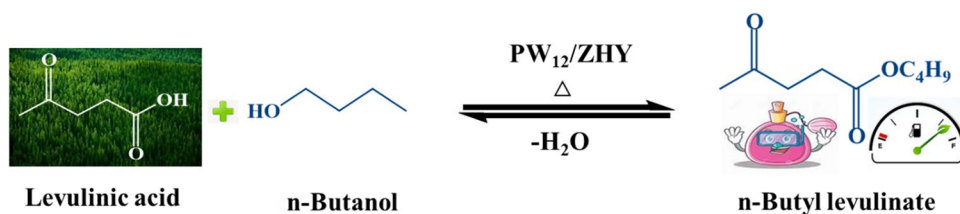


Fig. 8 a Effect of % loading of PW_{12} . Mole ratio: 1:2. Catalyst amount: 25 mg. Temperature: 90 °C. Time: 8 h. **b** Effect of mole ratio. Catalyst amount: 25 mg. Temperature: 90 °C. Time: 8 h. **c** Effect of catalyst amount. Mole ratio: 1:2. Temperature: 90 °C. Time:

8 h. **d** Effect of temperature. Mole ratio: 1:2. Catalyst amount: 25 mg. Time: 8 h. **e** Effect of time. Mole ratio: 1:2. Catalyst amount: 25 mg. Temperature: 90 °C

initial substrates at higher time. The % conversion initially decreased to 77%. Therefore, there was no such increase of % conversion from 10 to 12 h. Hence, 8 h is optimized.

Furthermore, to better understand the catalytic activity, we have also carried out reactions at higher temperature with lesser time. At 110 °C, the reaction proceed well even at lesser time. The % increases from 67 to 98% with the selectivity of 97–100% by varying it from 2 to 6 h. The reaction gave 99% conversion with the complete selectivity in 8 h. As our focus is to achieve good results in mild reaction conditions, we avoided higher temperature.

The optimized conditions for maximum % conversion (88%) and selectivity of ester (99%) are as follows: mole ratio of acid to alcohol 1:2, catalyst amount 25 mg (active amount of PW₁₂ 5.77 mg), reaction temperature 90 °C, and time 8 h). Turnover frequency (TOF) was calculated by using the following formulas, found to be 425 h⁻¹. $TOF = \text{number of moles of product} / [\text{number of moles of catalyst} \times \text{reaction time (h)}]$. Number of moles of catalyst was calculated by taking the active amount of PW₁₂.

Also, TOF was calculated using these reaction conditions: mole ratio of acid to alcohol 1:2, catalyst amount 25 mg, reaction temperature 90 °C, and time 2 h, which gives 45% conversion of levulinic acid with 89% selectivity of n-butyl levulinate. It was found to be 811 h⁻¹.

3.3 Leaching and hot filtration experiment

In the leaching as well as hot filtration test, no blue colouration was observed which indicates the absence of leaching of PW₁₂ from the support ZHY.

3.4 Kinetics: determination of activation energy (Ea)

A detailed kinetic study was carried out in a temperature range of 70 to 100 °C at time intervals of 4, 6, and 8 h under optimized conditions, where the % conversion of levulinic acid is $\geq 50\%$. For each temperature, the rate constant was calculated graphically [51] for 1st order [$\log a(a-x)$ vs time] as well as for 2nd order ($1/(a-x)$ vs time) and found to follow 2nd order (Table 4). Supplementary

Table 4 Rate constants k (M⁻¹ min⁻¹) at different temperatures (% conversion $\geq 50\%$) and activation energy (Ea)

Temperature (K)	Rate constant k (M ⁻¹ min ⁻¹)	Activation energy Ea (kJ/mol)
343	2.98×10^{-4}	80
353	1.04×10^{-3}	
363	2.28×10^{-3}	
373	3.03×10^{-3}	

Fig. S1 shows the plot of $1/(a-x)$ vs time at different temperatures, and the obtained rate constant is the value of slope. The straight line and values of $R^2 \geq 0.95$ show the reaction is followed by second order. For any heterogeneous system, activation energy plays a very important role. The activation energy was calculated from the graph of $\ln k$ vs $1/T$ (Fig. 9a) using the Arrhenius equation. It was found to be 80 kJ/mol. In chemical kinetics, it is believed that kinetic studies at higher % conversion may tend to leave reaction to thermodynamic equilibrium. To justify this, we have carried out the kinetic experiments keeping $\leq 50\%$ conversion of levulinic acid in a temperature range of 70 to 100 °C at time intervals of 0.5, 1, 1.5, 2, and 3 h. The rate constants were calculated graphically (Supplementary Fig. S2) for the same is enumerated in Table 5. Figure 9b approved that there were no such complications arise in the present study. Also, the values of activation energy are quite similar, i.e. 80 and 78.92 kJ/mol for kinetic studies at higher as well as lower % conversion respectively. In case of liquid phase reactions using heterogeneous catalyst, it is important to know whether the reaction is limited by diffusion regime, or it is governed by a chemical step. Hence, it is necessary to calculate energy of activation. It is already reported that if the activation energy lies in the range 10–15 kJ/mol, then the reaction is said to follow diffusion regime, and if the activation energy is found to be more than 25 kJ/mol, then the reaction is governed truly by chemical step [52]. The calculated activation energy is greater than 25 kJ/mol and confirms that the reaction is truly governed by a chemical step.

3.5 Control experiments

The results of control experiments are illustrated in Table 6. ZHY gives 53% conversion along with 95% selectivity of ester, whereas PW₁₂ gives complete conversion as well as selectivity. However, it should be noted that PW₁₂ behaves as a homogeneous catalyst, completely soluble in the reaction medium making separation very difficult and restrict the regeneration of catalyst. At the same time, PW₁₂/ZHY gives 88% conversion and 99% selectivity of ester with the advantage of being heterogenous with the synergy of Bronsted as well as Lewis acidity. Thus, we are succeeded to synthesize a catalyst which is truly heterogeneous in nature.

3.6 Regeneration of catalyst and its characterization

The regeneration experiments were carried out, and the results are shown in Fig. 10. The catalyst showed consistent activity with negligible change in the rate of conversion and selectivity of the desired ester up to three consecutive cycles. This suggests no leaching of PW₁₂ and hence gives nearly

Fig. 9 **a** Plot of $\ln k$ vs $1/T$ (% conversion $\geq 50\%$). **b** Plot of $\ln k$ vs $1/T$ (% conversion $\leq 50\%$)

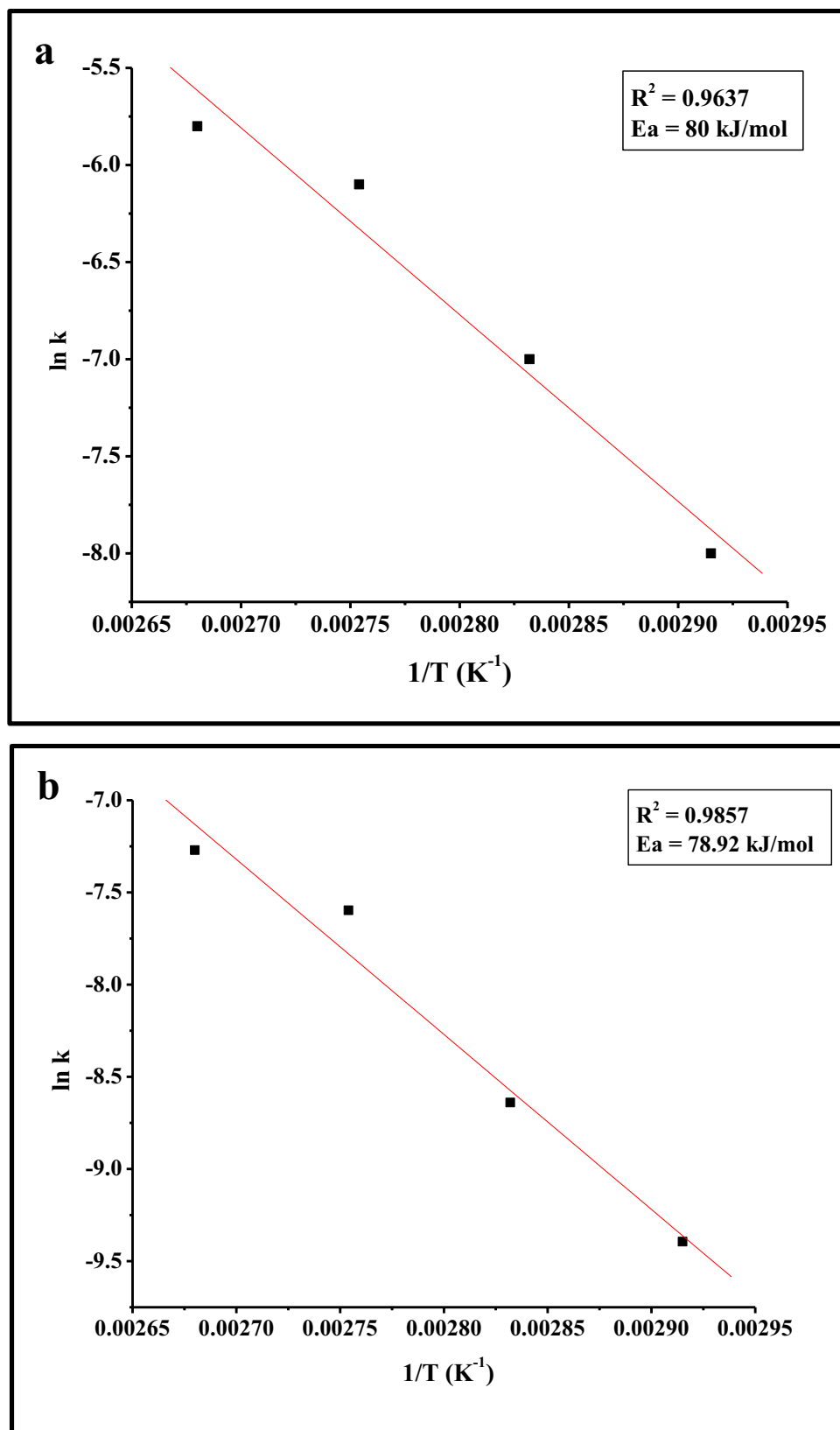


Table 5 Rate constants k ($M^{-1} \text{ min}^{-1}$) at different temperatures (% conversion $\leq 50\%$) and activation energy (E_a)

Temperature (K)	Rate constant k ($M^{-1} \text{ min}^{-1}$)	Activation energy E_a (kJ/mol)
343	8.32×10^{-5}	78.92
353	1.77×10^{-4}	
363	5.02×10^{-4}	
373	6.96×10^{-4}	

Table 6 Control experiments

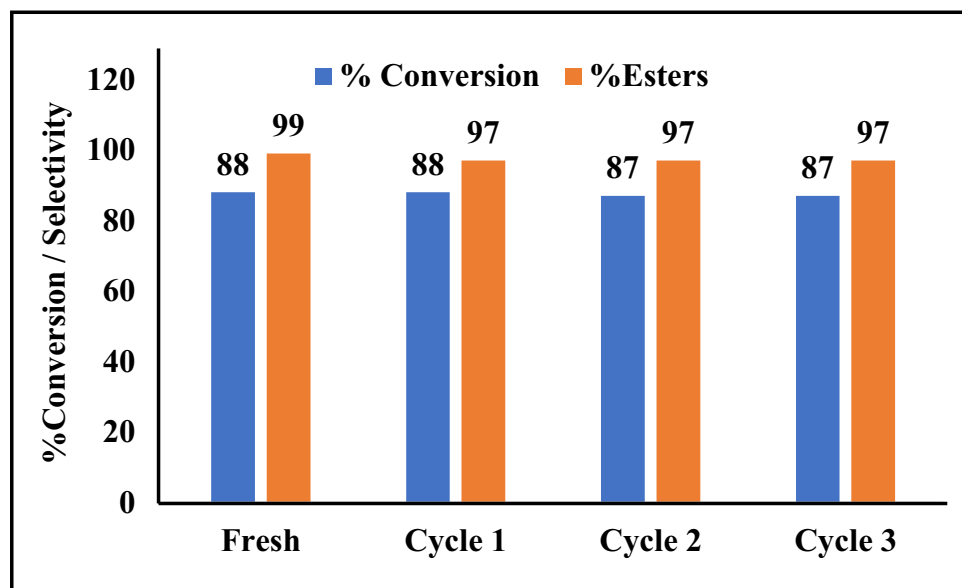
Catalyst	% conversion	% Selectivity of esters
¹ ZHY	53	95
² PW ₁₂	100	100
³ PW ₁₂ /ZHY	88	99

Reaction conditions: mole ratio 1:2 (levulinic acid: n-butanol), reaction temperature 90 °C, reaction time: 8 h. Catalyst amount 1 = 19.23 mg, 2 = 5.77 mg (active amount of PW₁₂), 3 = 25 mg

constant activity up to three cycles. Furthermore, the catalyst was characterized by acidity measurements, BET and FT-IR.

The total acidity of regenerated catalyst (1.50 mmol/g) was found to be good agreement with that of fresh catalyst (1.57 mmol/g). The N₂ sorption isotherms (Fig. 11) for both fresh and regenerated catalyst demonstrate identical isotherms support the sustainability of catalyst. Additionally, in FT-IR analysis (Fig. 12), the presence of all the characteristic bands of Keggin unit and that of the support indicates the stability and firm interaction of PW₁₂ with ZHY.

Fig. 10 Regeneration experiments: reaction conditions. Mole ratio 1:2 (levulinic acid: n-butanol). Catalyst amount 25 mg. Active amount of PW₁₂: 5.77 mg. Temperature 90 °C. Time: 8 h



3.7 Relative reactivity of different acids and alcohols

Esterification of levulinic acid with different alcohols (C3 to C8) was carried out, and results are shown in Fig. 13. It is very impressive that the catalyst shows % conversion in a range of 67–97% and selectivity of almost $\geq 90\%$ towards all the synthesized esters. It is clear from Fig. 13 that % conversion decreases with the increase in the carbon chain length of primary alcohols. Secondary as well as tertiary alcohols have less conversion as compared to primary alcohols. The reactivity of the alcohols follows the expected trend: primary > secondary > tertiary alcohols [53]. A decrease in the reactivity of secondary, tertiary, and branched alcohols may assign to steric hindrance on hydroxyl group of the alcohol, which effectively reduces the nucleophilic attack of that on carbonyl carbon of the carboxylic acid group in levulinic acid. It is known that steric hindrance is the slowing of reactions due to steric bulk, blocking the approach of carboxylic acid in esterification system. Also, steric hindrance can be seen when the molecules surrounding an active site unintentionally shield it due to the way they are situated around it. A steric hindrance is also responsible for lower conversion in primary alcohols having longer carbon chain length. It is worth to note down that in literature, mainly in patents, the synthesis of propyl levulinate is not widely studied, and present catalyst gives attractive result for the same (96% conversion and 95% selectivity). It should also be noted that very few reports are available on esterification of levulinic acid with longer chain alcohols (C5 to C8) using heterogeneous catalysts [54–56], and especially, the

Fig. 11 Nitrogen adsorption–desorption isotherms of **a** PW₁₂/ZHY and **b** R-PW₁₂/ZHY

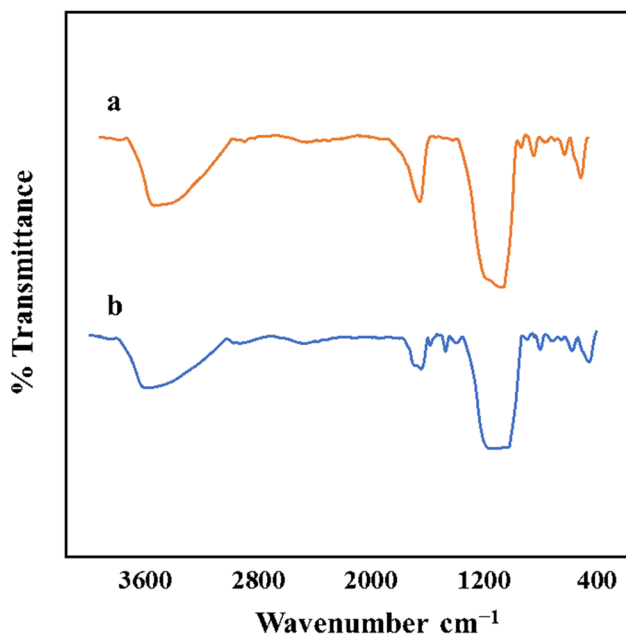
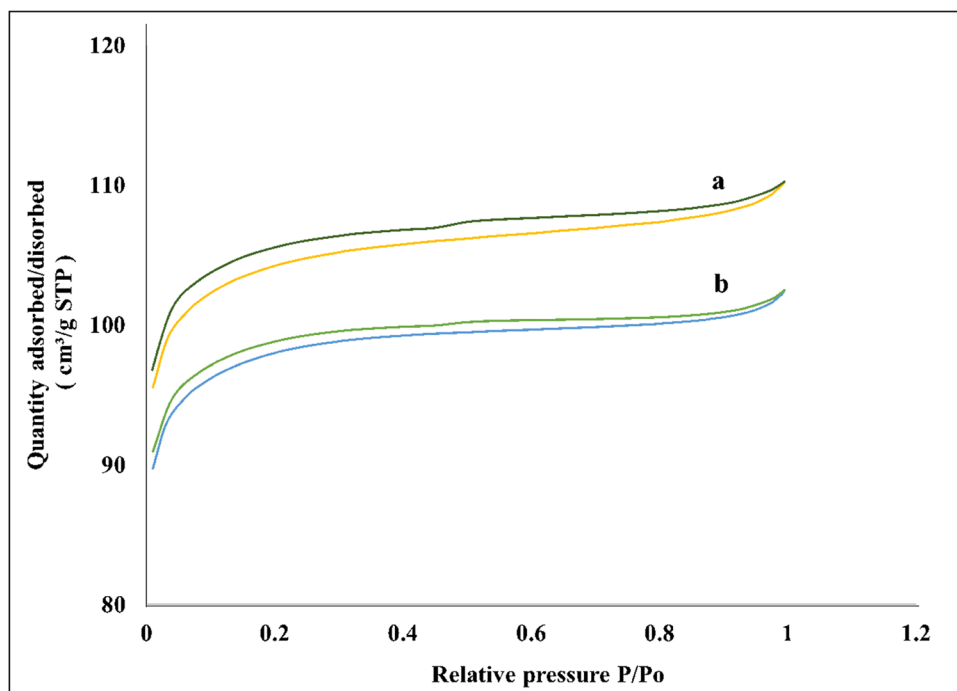


Fig. 12 FT-IR spectra of **a** PW₁₂/ZHY and **b** R-PW₁₂/ZHY

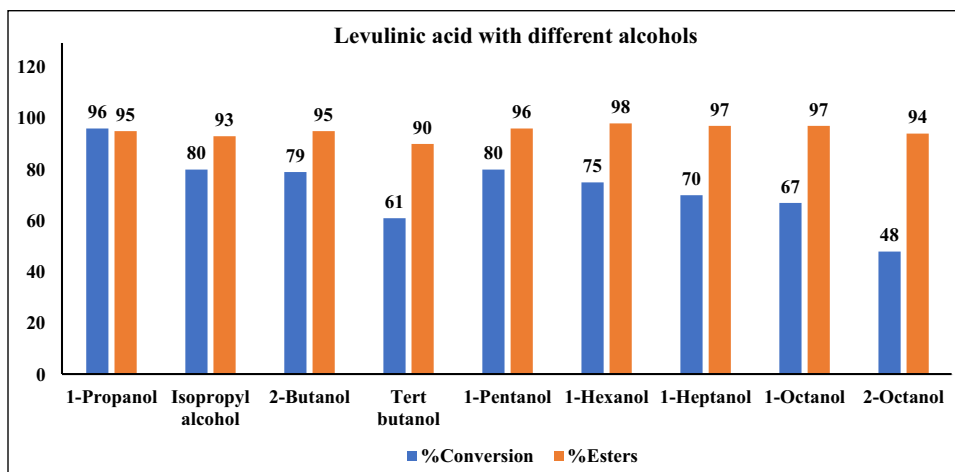
synthesis of pentyl levulinate is the subject of intensive research, as the literature has reported its synthesis by using ionic liquids [54]. It is noteworthy that, amongst these alkyl levulinates, most of levulinates have superb commercial applications, mostly in fuel blending. On the other hand, esterification of some bio-based carboxylic acids with n-butanol was also performed (Fig. 14). All

are straight-chain aliphatic acids that converted to the corresponding esters with a good % conversion (50–98%) under optimized conditions. Malonic acid and monoacids (palmitic acid and lauric acid) gave complete selectivity on the esterification with n-butanol. However, di-acids (fumaric acid, adipic acid, and succinic acid) showed dual selectivity of monoesters as well as diesters and difficult to achieve good selectivity for desired ester, i.e. diesters. For example, in case of succinic acid, few heterogeneous catalysts have been reported [57–59] with excellent conversion with low selectivity for diester, either in the presence of solvent or at comparatively higher temperatures (> 100 °C) with higher catalyst amount. In contrast, the present catalyst proves to work effectively at a lower temperature (90), using low catalyst amount and without solvent towards good selectivity (40%) for diester. The importance of data can be explained in terms of the strong Bronsted acidity of PW₁₂. It should be noted that increasing the Bronsted acidity via higher loading of active species or higher catalyst amount may further increase the diesterification. Thus, the catalyst comes out with distinctive reactivity towards formation of respective esters and explores its versatile catalytic approach towards the acids.

3.8 Comparison with reported catalysts

It is seen from Table 7 that the present catalyst is superior in terms of the catalyst amount as well as TOF amongst all. It is interesting to note down the difference in activity

Fig. 13 Esterification of levulinic acid with different alcohols over PW₁₂/ZHY. Reaction conditions. Mole ratio: 1:2. Catalyst amount: 25 mg. Temperature: 90 °C. Time: 8 h



of entries 4 and 5, instead of the presence of similar active species, i.e. PW₁₂, which PW₁₂/ZHY is better than PW₁₂/MCM-22 in terms of % conversion. This can be explained on the basis of nature of the support. It is well known that support does not play always merely a mechanical role in terms of surface area as well as the stability of the active species, but it can also modify the catalytic properties of the same, i.e. PW₁₂. ZHY has larger surface area (560 m²/g) as well as higher acidity (3.3 meqg⁻¹) than MCM-22 (surface area — 344 m²/g, acidity — 1.4 meqg⁻¹) Hence, ZHY offers better availability for PW₁₂ to interact. Furthermore, ZHY has less Al framework than that of MCM-22. Accordingly, PW₁₂/ZHY contains higher strong acidic sites (5.8 meqg⁻¹), while PW₁₂/MCM-22 contains 2.8 meqg⁻¹, in good agreement for the higher activity hence superiority.

The present catalyst has also been compared with the classical ion-exchange resins. In 2016, J. Tejero et al. have studied various acidic ion-exchange resins to synthesize n-butyl levulinate (entries 5 to 12). They have carried out the experiments

in a stainless-steel autoclave operated in batch mode with an electrical furnace controlling at 2.5 MPa using the reaction conditions temperature 80 °C, acid to alcohol molar ratio 1:3, catalyst amount 0.0004 g, and time 8 h with % conversion ranged from 64 to 94%. In the very next year, Ramli et al. have reported synthesis of n-butyl levulinate (55.3% conversion of levulinic acid) over an ion-exchange resin, Amberlyst-15 (entry 13) at temperature of 117.7 °C, acid to alcohol molar ratio 1:20, catalyst amount 0.348 g, and time 5 h. On a viewpoint of cost economy, the present catalyst is superior as the experiments were performed without any high-cost equipment as well as at lower temperature. Thus, even though classical resins are cheaper, the used harsh conditions make them economically less attractive. On the other hand, proposing a new catalyst, prepared with a specific route, would surely affect the economy of the process in terms of costs as synthesis of levulinates were carried out under mild conditions such lower temperature/catalyst amount/mole ratio of acid to alcohol and most importantly in a simple batch reactor.

Fig. 14 Esterification of different bio-platform molecules with n-butanol over PW₁₂/ZHY. Reaction conditions. Mole ratio: 1:2. Catalyst amount: 25 mg. Temperature: 90 °C. Time: 8 h

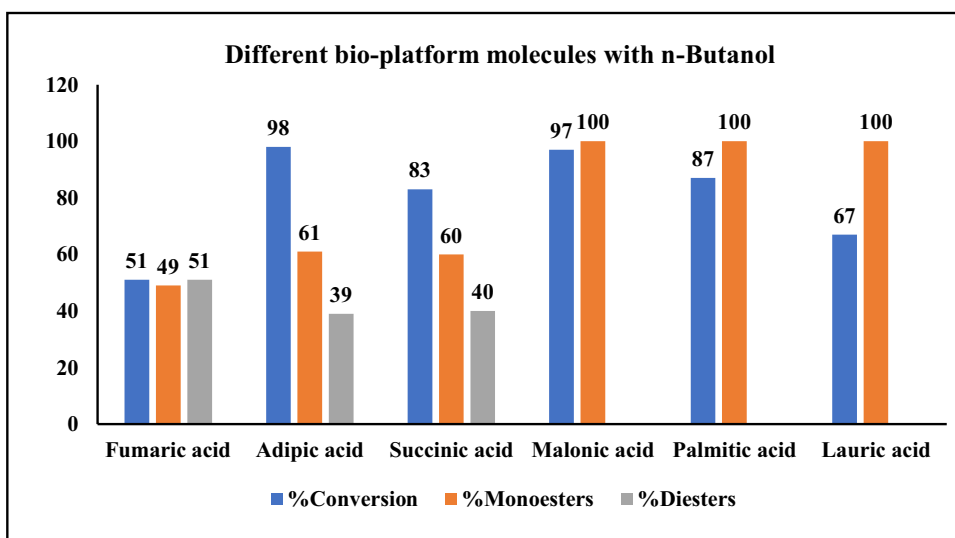


Table 7 Comparison with reported supported 12-tungstophosphoric acid as well as ion-exchange resins

Entry	Catalyst	Reaction conditions Mole ratio/catalyst amount(g)/temp. °C/ time (h)	% conv	TOF h ⁻¹	Reference
1	(NH ₄) _{0.5} Ag _{0.5} H ₂ PW	1:2/0.174/120/2	99	33	[27]
2	HPA/C-Sil-1	1:5/0.1/100/5	93	355	[28]
3	Fe ₃ O ₄ @SiO ₂ @SiO ₂ /TPA _{400N2}	1:2/0.1/80/7	95	15	[29]
4	PW ₁₂ /MCM-22	1:3/0.05/90/8	68	212	[30]
5	Amberlyst 46	1:3/0.004/80/8	63.9	-	[17]
6	Amberlyst 15	1:3/0.004/80/8	69.8	-	[17]
7	Amberlyst 35	1:3/0.004/80/8	70.9	-	[17]
8	Amberlyst 16	1:3/0.004/80/8	74.9	-	[17]
9	Amberlyst 36	1:3/0.004/80/8	78.1	-	[17]
10	Amberlyst 70	1:3/0.004/80/8	81.0	-	[17]
10	Amberlyst 39	1:3/0.004/80/8	86.6	-	[17]
12	Purolite CT-224	1:3/0.004/80/8	90.6	-	[17]
10	Dowex 50Wx8	1:3/0.004/80/8	81.3	-	[17]
11	Dowex 50Wx4	1:3/0.004/80/8	92.4	-	[17]
12	Dowex 50Wx2	1:3/0.004/80/8	93.6	-	[17]
13	Amberlyst 15	1:20/0.348/117.7/5	55.3	-	[60]
14	PW ₁₂ /ZHY	1:2/0.025/90/8	88	425	Present work

3.9 Reaction mechanism

The reaction mechanism for levulinic acid esterification with n-butanol is reported earlier by our group [30]. An adsorption of acid on the Brønsted acid sites of PW₁₂/ZHY leads to formation of protonated acid intermediate, and the electrophilicity of carbonyl carbon increases. At the same time, the carbonyl carbon is attacked by the nucleophilic oxygen of alcohol to form oxonium ion intermediate. The tetrahedral intermediate loses a water molecule and forms n-butyl levulinate. The Brønsted acidity of PW₁₂ as well as Lewis acid sites of ZHY plays a significant role in governing the reaction in forward direction. Also, the activity of ZHY is related to the formation of the transition state inside the channels [61]. Both the Lewis and Brønsted acidic sites of PW₁₂/ZHY enhance the proton accessibility and favour the overall reaction.

4 Conclusion

We succeeded to develop a solid acid catalyst with the possibility to upscale catalytic process by avoiding corrosion and waste liquid acid separation by combining the advantages of the high Bronsted acidity of 12-tungstophosphoric acid and the three-dimensional porous system of zeolite. The catalyst was characterized by various physicochemical methods to confirm incorporation of PW₁₂ into ZHY, intact structure, interaction, and stability. Under the optimized conditions, the catalyst

shows superb activity for the synthesis of n-butyl levulinate with almost complete selectivity, 99%. This method of production of n-butyl levulinate is solvent-free and sustainable as it is recycled and used up to multiple cycles, leading to the possibility of reaction system to upgrade renewable biomass, one of the main goals of green chemistry. Furthermore, the catalyst comes out with outstanding catalytic approach as compared to that of the reported catalysts for the same. To demonstrate its wide applicability, the catalyst was applied for different substrates including C3-C8 alcohols/bio-based carboxylic acids and outcomes with selectivity in the range of 49 to 100% showing its versatility. Especially, the synthesis of propyl levulinate is found to be very attractive with 96% conversion and 95% selectivity. The catalyst was also found to be very active towards the formation of diesters, due to the presence of strong Bronsted acidity arising from PW₁₂. As the influence of fuel blending of levulinates is of topmost researches, the present catalyst can be explored for the synthesis of large variety of bio-valuable products.

Supplementary Information The online version contains supplementary material available at <https://doi.org/10.1007/s13399-022-03279-2>.

Acknowledgements AP and MJ are thankful to the Department of Chemistry, The Maharaja Sayajirao University of Baroda for the infra-structural facilities and DST-FIST for BET surface area analysis. MJ is thankful to SHODH (ScHeme Of Developing High quality research, KCG/SHODH/2020-21/) for providing financial support.

Author contribution Anjali Patel, conceptualization, supervision, and writing — review and editing; Margi Joshi, formal analysis and investigation, methodology, and writing — original draft preparation; Shivani Sharma, preliminary experiments and analysis.

Data availability Supplementary information is available.

Declarations

Ethics approval Not applicable.

Consent to participate No conflicts, informed consent, or human or animal rights are applicable to this study.

Conflict of interest The authors declare no competing interests.

References

- Al-Shaal MG, Ciptonugroho W, Holzhäuser FJ, Mensah JB, Hausoul PJC, Palkovits R (2015) Catalytic upgrading of α -angelica lactone to levulinic acid esters under mild conditions over heterogeneous catalysts. *Catal Sci Technol* 5:5168–5173. <https://doi.org/10.1039/C5CY00446B>
- Luterbacher JS, Alonso DM, Dumesic JA (2014) Targeted chemical upgrading of lignocellulosic biomass to platform molecules. *Green Chem* 16:4816–4838. <https://doi.org/10.1039/C4GC01160K>
- Neves P, Antunes MM, Russo PA, Abrantes JP, Lima S, Fernandes A, Pillinger M, Rocha SM, Riberio MF, Valente AA (2013) Production of biomass-derived furanic ethers and levulinic acid esters using heterogeneous acid catalysts. *Green Chem* 15:3367–3376. <https://doi.org/10.1039/C3GC41908H>
- Krishnan V, McCalley JD (2016) The role of bio-renewables in national energy and transportation systems portfolio planning for low carbon economy. *Renew Energy* 91:207–223. <https://doi.org/10.1016/j.renene.2016.01.052>
- Jahangiri H, Santos J, Hornung A, Ouadi M (2021) Thermochemical conversion of biomass and upgrading of bio-products to produce fuels and chemicals BT - catalysis for clean energy and environmental sustainability. In: Pant KK, Gupta SK, Ahmad E (eds) *Biomass Conversion and Green Chemistry*, Springer International Publishing, Cham, pp 1: 1–47. <https://doi.org/10.1007/978-3-030-65017-9>
- Christensen E, Williams A, Paul S, Burton S, McCormick RL (2011) Properties and performance of levulinic acid esters as diesel blend components. *Energy Fuels* 25:5422–5428. <https://doi.org/10.1021/ef201229j>
- Dharne S, Bokade VV (2011) Esterification of levulinic acid to n-butyl levulinate over heteropolyacid supported on acid-treated clay. *J Nat Gas Chem* 20:18–24. [https://doi.org/10.1016/S1003-9953\(10\)60147-8](https://doi.org/10.1016/S1003-9953(10)60147-8)
- Maheria KC, Kozinski J, Dalai A (2013) Esterification of levulinic acid to n-butyl levulinate over various acidic zeolites. *Catal Lett* 143:1220–1225. <https://doi.org/10.1007/s10562-013-1041-3>
- Nandiwale KY, Bokade VV (2014) Esterification of renewable levulinic acid to n-butyl levulinate over modified H-ZSM-5. *Chem Eng Technol* 38:246–252. <https://doi.org/10.1002/ceat.201400326>
- Cirujano FG, Corma A, Ixamena FXL (2015) Conversion of levulinic acid into chemicals: synthesis of biomass derived levulinic acid esters over Zr-containing MOFs. *Chem Eng Sci* 124:52–60. <https://doi.org/10.1016/j.ces.2014.09.047>
- Peixoto AF, Soliman MMA, Pinto TV, Silva SM, Costa P, Alegria ECBA, Freire C (2021) Highly active organosulfonic aryl-silica nanoparticles as efficient catalysts for biomass derived biodiesel and fuel additives. *Biomass Bioenergy* 145:105936. <https://doi.org/10.1016/j.biombioe.2020.105936>
- Yang F, Tang J (2019) Catalytic upgrading of renewable levulinic acid to levulinic acid esters using perchloric acid decorated nanoporous silica gels. *ChemistrySelect* 4:1403–1409. <https://doi.org/10.1002/slct.201803608>
- Ramli NAS, Hisham NI, Amin NAS (2018) Esterification of levulinic acid to levulinic acid esters in the presence of sulfated silica catalyst. *Sains Malays* 47:1131–1138. <https://doi.org/10.17576/jsm-2018-4706-08>
- Chermahini AN, Nazari M (2017) Esterification of the levulinic acid with n-butyl and isobutyl alcohols over aluminum-containing MCM-41. *Fuel Process Technol* 167:442–450. <https://doi.org/10.1016/j.fuproc.2017.07.034>
- Pachamuthua MP, Srinivasanb VV, Karvembub R, Luquec R (2019) Preparation of mesoporous stannosilicates SnTUD-1 and catalytic activity in levulinic acid esterification. *Microporous Mesoporous Mater* 287:159–166. <https://doi.org/10.1016/j.micromeso.2019.05.061>
- Miao Z, Li Z, Zhao J, Si W, Zhou J, Zhuo S (2018) MoO₃ supported on ordered mesoporous zirconium oxophosphate: an efficient and reusability solid acid catalyst for alkylation and esterification. *Mol Catal* 444:10–21. <https://doi.org/10.1016/j.mcat.2017.10.028>
- Tejero MA, Ramírez E, Fité C, Tejero J, Cunill F (2016) Esterification of levulinic acid with butanol over ion exchange resins. *Appl Catal A Gen* 517:56–66. <https://doi.org/10.1016/j.apcata.2016.02.032>
- Trombettoni V, Bianchi L, Zupanec A, Porciello A, Cuomo M, Piermatti O, Marrocchi A, Vaccaro L (2017) Efficient catalytic upgrading of levulinic acid into alkyl levulinates by resin-supported acids and flow reactors. *Catalysts* 7:235. <https://doi.org/10.3390/catal7080235>
- Nakhate AV, Yadav GD (2016) Synthesis and characterization of sulfonated carbon based graphene oxide monolith by solvothermal carbonization for esterification and unsymmetrical ether formation. *ACS Sustain Chem Eng* 4:1963–1973. <https://doi.org/10.1021/acssuschemeng.5b01205>
- Zhou S, Jiang D, Liu X, Chen Y, Yin D (2018) Titanate nanotubes-bonded organosulfonic acid as solid acid catalyst for synthesis of butyl levulinate. *RSC Adv* 8:3657–3662. <https://doi.org/10.1039/C7RA12994G>
- Mao FF, Zhao W, Tao DJ, Liu X (2020) Highly efficient conversion of renewable levulinic acid to n-butyl levulinate catalyzed by sulfonated magnetic titanium dioxide nanotubes. *Catal Lett* 150:2709–2715. <https://doi.org/10.1007/s10562-020-03177-0>
- Emrah Altuntepe E, Emel'yanenko VN, Forster-Rodgers M, Sadowski G, Verevkin SP, Held C (2017) Thermodynamics of enzyme-catalyzed esterifications: II. Levulinic acid esterification with short-chain alcohols. *Appl Microbiol Biotechnol* 101:7509–7521. <https://doi.org/10.1007/s00253-017-8481-4>
- Zhou L, Hea Y, Maa L, Jianga Y, Huang Z, Yina L, Gao J (2018) Conversion of levulinic acid into alkyl levulinates: using lipase immobilized on meso-molding three-dimensional macroporous organosilica as catalyst. *Bioresour Technol* 247:568–575. <https://doi.org/10.1016/j.biortech.2017.08.134>
- Badgujar KC, Bhanage BM (2015) Thermo-chemical energy assessment for production of energy-rich fuel additive compounds by using levulinic acid and immobilized lipase. *Fuel Process Technol* 138:139–146. <https://doi.org/10.1016/j.fuproc.2015.05.015>
- Tian Y, Zhang R, Zhao W, Wen S, Xiang Y, Liu X (2020) A new sulfonic acid-functionalized organic polymer catalyst for

- the synthesis of biomass-derived alkyl levulinates. *Catal Lett* 150:3553–3560. <https://doi.org/10.1007/s10562-020-03253-5>
26. Wang H, Lu Y, Liu H, Yin Y, Liang J (2020) Preparation and application of magnetic nano-solid acid catalyst Fe_3O_4 -PDA- SO_3H . *Energies* 13:1484. <https://doi.org/10.3390/en13061484>
 27. Zhou X, Li ZX, Zhang C, Gao XP, Dai YZ, Wang GY (2016) Efficient conversion of renewable levulinic acid to n-butyl levulinate catalyzed by ammonium and silver co-doped phosphotungstic acid. *J Mol Catal A Chem* 417:71–75. <https://doi.org/10.1016/j.molcata.2016.03.006>
 28. Manikandan K, Cheralathan KK (2017) Heteropoly acid supported on silicalite-1 possessing intracrystalline nanovoids prepared using biomass – an efficient and recyclable catalyst for esterification of levulinic acid. *Appl Catal A Gen* 547:237–247. <https://doi.org/10.1016/j.apcata.2017.09.007>
 29. Escobar AM, Blanco MN, Martínez JJ, Cubillos JA, Romanelli GP, Pizzio LR (2019) Biomass derivative valorization using nano core-shell magnetic materials based on Keggin-heteropolyacids: levulinic acid esterification kinetic study with N-butanol. *J Nanomater* 2019:5710708. <https://doi.org/10.1155/2019/5710708>
 30. Pithadia D, Patel A, Hatiya V (2022) 2-Tungstophosphoric acid anchored to MCM-22, as a novel sustainable catalyst for the synthesis of potential biodiesel blend, levulinate ester. *Renew Energy* 187:933–943. <https://doi.org/10.1016/j.renene.2022.01.106>
 31. Chena Y, Zhanga X, Dong M, Wua Y, Zhengc G, Huang a J, Guana X, Zheng X (2016) MCM-41 immobilized 12-silicotungstic acid mesoporous materials: structural and catalytic properties for esterification of levulinic acid and oleic acid. *J Taiwan Inst Chem Eng* 61:147–155. <https://doi.org/10.1016/j.jtice.2015.12.005>
 32. Luana Q, Liua L, Gong a S, Lua J, Wang X, Lv D (2018) Clean and efficient conversion of renewable levulinic acid to levulinate esters catalyzed by an organic-salt of $\text{H}_4\text{SiW}_{12}\text{O}_{40}$. *Pross Saf Environ Prot* 117:341–349. <https://doi.org/10.1016/j.psep.2018.05.015>
 33. Misono M (1993) Catalytic chemistry of solid polyoxometalates and their industrial applications. *Mol Eng* 3:193–203. <https://doi.org/10.1007/BF00999633>
 34. Cejka J, Centi G, Pariente JP, Roth WJ (2012) Zeolite-based materials for novel catalytic applications: opportunities, perspectives and open problems. *Catal Today* 179:2–15. <https://doi.org/10.1016/j.cattod.2011.10.006>
 35. Lanzafame P, Barbera K, Papanikolaou G, Perathoner S, Centi G, Migliori M, Catizzone E, Giordano G (2017) Comparison of H^+ and NH_4^+ forms of zeolites as acid catalysts for HMF etherification. *Catal Today* 304:97–102. <https://doi.org/10.1016/j.cattod.2017.08.004>
 36. Li G, Pidko EA (2019) The nature and catalytic function of cation sites in zeolites: a computational perspective. *ChemCatChem* 11:134–156. <https://doi.org/10.1002/cctc.201801493>
 37. Liu Z, Shi C, Wu D, He S, Ren B (2016) A simple method of preparation of high silica zeolite Y and its performance in the catalytic cracking of cumene. *J Nanotechnol* 2016:1486107. <https://doi.org/10.1155/2016/1486107>
 38. Sahu HR, Rao GR (2000) Characterization of combustion synthesized zirconia powder by UV- vis, IR and other techniques. *Bull Mater Sci* 23:349–354. <https://doi.org/10.1007/BF02708383>
 39. Ferreira P, Fonseca IM, Ramos AM, Vital J, Castanheiro JE (2010) Valorisation of glycerol by condensation with acetone over silica-included heteropolyacids. *Appl Catal B* 98:94–99. <https://doi.org/10.1016/j.apcatb.2010.05.018>
 40. Patel A, Pithadia D (2020) Low temperature synthesis of bio-fuel additives via valorisation of glycerol with benzaldehyde as well as furfural over a novel sustainable catalyst, 12-tungstosilicic acid anchored to ordered cubic nano-porous MCM-48. *Appl Catal A Gen* 602:117729. <https://doi.org/10.1016/j.apcata.2020.117729>
 41. Ramli NAS, Amin NAS (2014) Fe/HY zeolite as an effective catalyst for levulinic acid production from glucose: characterization and catalytic performance. *Appl Catal B* 163:487–498. <https://doi.org/10.1016/j.apcatb.2014.08.031>
 42. Deltcheff CR, Fournier M, Franck R, Thouvenot R (1983) Vibrational investigations of polyoxometalates. 2. Evidence for anion-anion interactions in molybdenum(VI) and tungsten(VI) compounds related to the Keggin structure. *Inorg Chem* 22:207–216. <https://doi.org/10.1021/IC00144A006>
 43. Ayad Z, Hussein HQ, Tabbakh BAA (2020) Synthesis and characterization of high silica HY zeolite by basicity reduction. *AIP Conf Proc* 2213:020168. <https://doi.org/10.1063/5.0000278>
 44. dos Santos de Castro PR, Maia AAB, Angélica RS (2019) Study of the thermal stability of faujasite zeolite synthesized from Kaolin waste from the Amazon. *Mater Res* 22:e20190321. <https://doi.org/10.1590/1980-5373-MR-2019-0321>
 45. Highfield JG, Moffat JB (1984) Characterization of 12-tungstophosphoric acid and related salts using photoacoustic spectroscopy in the infrared region II. Interactions with Pyridine. *J Catal* 89:185–195. [https://doi.org/10.1016/0021-9517\(84\)90296-3](https://doi.org/10.1016/0021-9517(84)90296-3)
 46. Freitas EF, Araújo AAL, Paiva MF, Dias SCL, Dias JA (2018) Comparative acidity of BEA and Y zeolite composites with 12-tungstophosphoric and 12-tungstosilicic acids. *Mol Catal* 458:152–160. <https://doi.org/10.1016/j.mcat.2018.03.005>
 47. Okuhara T, Mizuno N, Misono M (1996) Catalytic chemistry of heteropoly compounds. *Adv Catal* 41:113–252. [https://doi.org/10.1016/S0360-0564\(08\)60041-3](https://doi.org/10.1016/S0360-0564(08)60041-3)
 48. Mizunon N, Misono (1987) M pore structure and surface area of $\text{Cs}_x\text{H}_{3-x}\text{PM}_{12}\text{O}_{40}$ ($x=0-3$, $M=W, \text{Mo}$). *Chem Lett* 16:967–970. <https://doi.org/10.1246/cl.1987.967>
 49. Badgujara KC, Badgujara VC, Bhanage BM (2020) A review on catalytic synthesis of energy rich fuel additive levulinate compounds from biomass derived levulinic acid. *Fuel Process Technol* 197:106213. <https://doi.org/10.1016/j.fuproc.2019.106213>
 50. Schüth F, Ward MD, Buriak JM (2018) Common pitfalls of catalysis manuscripts submitted to chemistry of materials. *Chem Mater* 30:3599–3600. <https://doi.org/10.1021/acs.chemmater.8b01831>
 51. Puri BR, Sharma LR, Pathania MS (1962) Principles of physical chemistry. Vishal Publishing Co., p 1033–1111
 52. Bond GC (1974) Heterogeneous catalysis: principles and applications. Clarendon Press, Oxford, p 4
 53. Liang J, Liang Z, Zou R, Zhao Y (2017) Heterogeneous catalysis in zeolites, mesoporous silica, and metal-organic frameworks. *Adv Mater* 29:1701139. <https://doi.org/10.1002/adma.201701139>
 54. Przepis M, Matuszek K, Chrobok A, Swadźba-Kwaśny M, Gillner D (2020) Inexpensive and tuneable protic ionic liquids based on sulfuric acid for the biphasic synthesis of alkyl levulinates. *J Mol Liq* 308:113166–113173. <https://doi.org/10.1016/j.molliq.2020.113166>
 55. Mortazavi M, Chermahini AN, Mohammadbagheri Z (2019) Synthesis of hexyl levulinate as a potential fuel additive from levulinic acid over a solid acid catalyst. *J Environ Chem Eng*. <https://doi.org/10.1016/j.jece.2019.103420>
 56. Gupta SSR, Kantam ML (2019) Catalytic conversion of furfuryl alcohol or levulinic acid into alkyl levulinates using a sulfonic acid-functionalized hafnium-based MOF. *Catal Commun* 124:62–66. <https://doi.org/10.1016/J.CATCOM.2019.03.003>
 57. Alamdari FR, Niri MN, Hazarkhanian H (2018) A novel hydrogen-bonded silica-supported acidic ionic liquid: an efficient, recyclable and selective heterogeneous catalyst for the synthesis of diesters. *J Chem Sci* 130:48. <https://doi.org/10.1007/s12039-018-1454-z>

58. Lown AL, Peereboom L, Mueller SA, Anderson JE, Miller DJ, Lira CT (2014) Cold flow properties for blends of biofuels with diesel and jet fuels. *Fuel* 117:544–551. <https://doi.org/10.1016/j.fuel.2013.09.067>
59. Jing C, Jinhua L, Zhongxie D, Yuehua W, Zhen L, Min J, Xiaoqian R (2018) Lewis acid sites of Mg²⁺-modified polystyrene sulfonic acid resin catalysis for synthesis of dibutyl succinate. *Quím Nova* 41:613–618. <https://doi.org/10.21577/0100-4042.20170230>
60. Ramli NAS, Zaharudin NH, Amin NAS (2017) Esterification of renewable levulinic acid to levulinate esters using amberlyst-15 as a solid acid catalyst. *J Teknol* 79:137–142. <https://doi.org/10.11113/jt.v79.8095>
61. Lutz W (2014) Zeolite Y: synthesis, modification, and properties—a case revisited. *Adv Mater Sci Eng* 2014:724248. <https://doi.org/10.1155/2014/724248>

Publisher's note Springer Nature remains neutral with regard to jurisdictional claims in published maps and institutional affiliations.

Springer Nature or its licensor holds exclusive rights to this article under a publishing agreement with the author(s) or other rightsholder(s); author self-archiving of the accepted manuscript version of this article is solely governed by the terms of such publishing agreement and applicable law.